Acoustics at an interface : promoting the Lagrange picture

Martin Devaud, Thierry Hocquet

Acoustics at an interface : promoting the Lagrange picture

Martin Devaud*
Université Denis Diderot, Sorbonne Paris Cité, MSC, UMR 7057 CNRS,
10 rue Alice Domon et Léonie Duquet, 75013 PARIS, France

Thierry Hocquet
Université Denis Diderot, Sorbonne Paris Cité, MSC, UMR 7057 CNRS,
10 rue Alice Domon et Léonie Duquet, 75013 PARIS, France and
Université Pierre et Marie Curie - Paris 6, 4 place Jussieu, 75005 PARIS, France

In Fluid Mechanics, the Euler description is widely taught and used at the undergraduate level, and the Lagrange description is rather presented as an alternative peculiarity. In this paper, it is argued that, as far as acoustics is envisaged, the Lagrange description occurs to offer a more suitable approach as well from a pedagogical viewpoint as from a technical one. Sound generation by a pulsating source and reflection/transmission at an interface are discussed in this respect.

I. INTRODUCTION

Whenever an acoustic wave travels through an interface from one medium to another, it splits into a reflected and a transmitted wave, exactly as a light beam would do when crossing the boundary between two media with different refractive indices. In the latter optical case, it is neither conceptually embarrassing nor technically difficult to derive the reflection and transmission coefficients at the interface. Using the standard continuity relations of the electromagnetic fields at the boundary, one easily determines the reflected and transmitted fields as a function of the incident ones. It is noteworthy that, in the optical case, the problem is particularly simple in this sense that the geometry of the boundary on the one hand, and the electromagnetic state of the optical media on the other hand, are utterly disconnected. More precisely, the position of the boundary is independent of the electric (or magnetic) polarization of the media: the optical wave does not entail any (macroscopic) motion of the the media. In the acoustic case, things are not that simple, as illutrated in figure 1: two different fluids – say 1 and 2 – are separated *at rest* by the (infinite) plane $x = 0$. Let us consider now a plane pressure wave propagating from $x = -\infty$ in fluid 1 towards the boundary. As well known, this incident wave splits at the interface in two parts: a reflected wave, travelling back to $x = -\infty$ through medium 1, and a transmitted wave, travelling towards $x = +\infty$ through medium 2. It is a time-honored undergraduate level exercice to determine the reflection and the transmission coefficients at the interface. In principle, the answer is easy: one equalizes the fluid pressures

$$P_1(\text{interface}) = P_2(\text{interface}) \tag{1a}$$

and the fluid velocities

$$\vec{v}_1(\text{interface}) = \vec{v}_2(\text{interface}), \tag{1b}$$

which provides two equations enabling us to calculate both coefficients. The above process is undoubtedly correct, but raises a nontrivial difficulty: *where* is the interface? At $x = 0$? Certainly not, since the interface *itself* moves back and forth, due to the wave motion. As a matter of fact, the $x = 0$ plane spends half time in medium 1, half time in medium 2. Of course, locating the interface at $x = 0$ is the best *approximation*, and it leads to the correct values of the reflection and transmission coefficients, but it should be regarded as but an order-zero approximation.

Contrary to the optical case evoked above, the geometric position of the boundary and the acoustic vibration are entangled. When dealing with the situation illustrated in figure 1, the difficulty we meet originates in our attempt

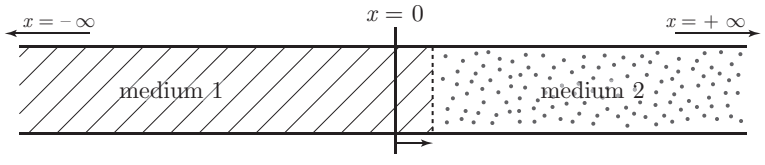

FIG. 1: Medium 1 and medium 2 are separated at rest by the plane $x = 0$. When a pressure wave propagates, the interface does not remain at $x = 0$, but moves back and forth on either side of the plane $x = 0$. In the Euler description, locating the interface at $x = 0$ appears as an order-zero approximation.

of using the formalism adopted in Fluid Mechanics, and known as the Euler description: to put it briefly, a (usely Galilean) reference frame is defined. At a given point $\vec{r}$ of this frame, and at time t, the physical state of the fluid is described by a set of parameters: mass density ρ, pressure P, fluid velocity (with respect to the frame) $\vec{v}$, temperature T and so on. So that one deals with a set of (coupled) continuous fields $\rho(\vec{r},t)$, $P(\vec{r},t)$, $\vec{v}(\vec{r},t)$, $T(\vec{r},t)$, *etc.* For instance, in absence of any external force (gravity or other), and neglecting viscosity for the sake of simplicity, the movement of an inviscid fluid is ruled by the well-known Euler equation

$$\rho(\vec{r},t)\left(\frac{\partial \vec{v}}{\partial t}+(\vec{v}\cdot\overrightarrow{\text{grad}})\,\vec{v}\right)=-\overrightarrow{\text{grad}}\,P. \tag{2}$$

Such a description has many advantages. First, it is convenient to account for the dynamics of the fluid by means of *local* equations coupling fields, exactly as in the Electromagnetism domain. Second, the Euler description is particularly well adapted to situations in which the fluid really *flows*: when studying the stream of a river passing at some bridge, we are interested in the very behavior of the water under this bridge at a time t, whichever the origin or the past behavior of this water.

Nevertheless, the Euler description is not without a major drawback. Let us glance at equation (2). The left-hand side is obviously nonlinear in field $\vec{v}$, due to the $(\vec{v}\cdot\overrightarrow{\text{grad}})\,\vec{v}$ term: in contrast to the Maxwell equations, the Euler equation is nonlinear. In addition to the latter *explicit* nonlinearity, an *implicit* further nonlinearity hides in the mass density term as soon as the fluid is compressible, since $\rho(\vec{r},t)$ is *a priori* $\vec{v}$-dependent.

In textbooks,[1,2] when using the Euler description to teach Acoustics at the undergraduate level, a perturbative resolution of the Euler equation is implemented: expanding fields $\rho(\vec{r},t)$, $\vec{v}(\vec{r},t)$, $P(\vec{r},t)$ in increasing powers of the acoustic amplitude and restricting to the lowest significant order (namely order zero for the mass density and order one for the fluid velocity and the pressure), we are left with a linearized form of the Euler equation which can be easily handled. Such a linearization is argued to be justified as far as the fluid particle velocity is small compared to the wave phase velocity. In the same connection, the *equilibrium* position of the interface (namely $x=0$ in the situation illustrated in figure 1) is chosen to determine the reflection and transmission coefficients.

Although the above-recalled processes undoubtedly work, students are often left with the uncomfortable feeling that they do not perfectly master the approximations they have been led to make in the course of the calculation. In fact, the above-underlined difficulties of the Euler description can be (up to a point) overcome in an alternative framework, known as the Lagrange description.[3–5] It is noteworthy that such an alternative in the description of the physical state of a system is also encountered in the quantum formalism. For this reason, we shall henceforth deliberately substitute the word "picture" for "description": the Euler picture and the Lagrange picture are indeed, as outlined below, the exact transposition to fluid mechanics of the so-called "Schrödinger picture" and "Heisenberg picture" of quantum mechanics. It is precisely the aim of the present paper to sketch the main features of the Lagrange picture which is poorly taught in academic courses and scarcely used when studying acoustic propagation.

To begin with, what is it all about? The philosophy of the Lagrange picture can be outlined as follows. Contrary to the Euler picture, which, as recalled above, labels the geometric points of the reference frame disregarding the origin of the fluid elements passing through these points at time t, the Lagrange picture labels the fluid elements disregarding the exact position they occupy at time t. Let us detail hereafter how it works. With this aim, let us consider a fluid at some time t_0. We denote $\vec{r}_0$ the fluid element that is positioned at point $\vec{r}_0$ of the reference frame at time t_0. We shall henceforth keep this label $\vec{r}_0$ to denote this fluid element, whatever its further motion. Thus, at time t, the fluid element $\vec{r}_0$ will be found at some point $\vec{r}$ given by

$$\vec{r}(\vec{r}_0,t)=\vec{r}_0+\vec{u}(\vec{r}_0,t), \tag{3}$$

where $\vec{u}(\vec{r}_0,t)$ is the displacement of the fluid element $\vec{r}_0$ between times t_0 and t. The physical state of the fluid is still described by a set of continuous fields: mass density, pressure, velocity, temperature, *etc.* The correspondance between both pictures is very simple. Superscripts $\mathcal{E}$ and $\mathcal{L}$ respectively denoting "Euler" and "Lagrange", we have, quantity A standing for whichever parameter ρ, P, $\vec{v}$, T, *etc.*,

$$A^{\mathcal{E}}\big(\vec{r}(\vec{r}_0,t),t\big)=A^{\mathcal{L}}(\vec{r}_0,t), \tag{4}$$

with $\vec{r}(\vec{r}_0,t)$ given by (3). Concretely, the above equation (4) means that $A^{\mathcal{L}}(\vec{r}_0,t)$ denotes the actual value of parameter A as undergone at time t by the fluid element labeled $\vec{r}_0$ which is currently at point $\vec{r}_0+\vec{u}(\vec{r}_0,t)$ of the reference frame, *i.e.* $A^{\mathcal{L}}(\vec{r}_0,t)$ is *numerically* equal to $A^{\mathcal{E}}\big(\vec{r}(\vec{r}_0,t),t\big)$.

We show in the present paper that the Lagrange picture offers several advantages from a *technical* point of view. To begin with, this picture rids us of *spurious* nonlinearities (for instance, the pseudo nonlinearity associated with the

$(\vec{v}\cdot\overrightarrow{\text{grad}})\,\vec{v}$ term in the left-hand side of the Euler equation (2)), and enables us to index and classify *true* nonlinearities, allowing (should the occasion occur) perturbative resolutions of the field equations. Secondly, each fluid element d^3r_0 is, thermodynamically speaking, a *closed* system: no particle exchange with the outside occurs, except a possible – and neglected in this paper – matter diffusion. A third technical advantage of the Lagrange picture appears when dealing with interfaces co-moving with the fluid(s). This point will be illustrated in detail in subsections II B, II C, III B and III C.

Let us add that the Lagrange labeling of the fluid particles can be easily visualized using passive markers, designed to follow the flow without perturbing it in any way: they behave exactly as would behave a "painted" fluid particle. Observing the trajectories of the latter markers provides an experimental check for mathematical solutions or simulations and, besides, is of interest for environmental problems (see for instance[5]).

Teaching the Lagrange picture also offers some advantage from a *pedagogical* point of view. A very natural way indeed to introduce the continuous media dynamics consists in starting from a discrete description of matter: using Newton's Second Law, the dynamics of every fluid element is established, then merged into a continuous description (typically, in lattice dynamics, this continuous description naturally emerges when the conditions of the center of Brillouin zone propagation are fulfilled). In this respect, the bridge with the Euler picture is a bit more delicate (leading for instance to the spurious $(\vec{v}\cdot\overrightarrow{\text{grad}})\,\vec{v}$ nonlinearity mentioned above).

Nevertheless, our promotion of the Lagrange picture would be incomplete if we did not stress the following feature. Let us consider the position of a moving fluid at some initial time t_0. Labelling the different fluid elements by their position $\vec{r}_0$ with respect to the reference frame, we can of course choose a set of Cartesian coordinates: $\vec{r}_0(x_0, y_0, z_0)$. But, in the course of the subsequent motion, we will have to take the distortion of the fluid elements into account in order to write correctly the local balance equations (as (2) for instance, where both hand-sides have to be reconsidered in the framework of the Lagrange picture). Now, due to the *a priori* complex motion of the fluid, our coordinate system is no longer Cartesian at any time t, but *curvilinear* (of course, we should never have the same problem with the Euler picture, since then the choice of a Cartesian coordinate system to label the geometric points of the reference frame can be made *once for all*). For this reason, and for the sake of simplicity, we shall restrict this article to the study of the one-dimension case and, in the three-dimension case, to the mere spherical geometry.

With this general philosophy, we have organized the present paper as follows. In section II, we focus on the one-dimension problem. We illustrate our purpose with the calculation (subsection II A) of the exact solution of the sound propagation in a fluid with a linear extrapressure-to-dilatation thermodynamic relation. Then (subsection II B) we address the most simple following question: how do we calculate the acoustic wave generated by a load-speaker? We finish with the determination (subsection II C) of the reflection/transmission coefficients at an interface. Section III is devoted to the three-dimension case. After a quick overflight of the general situation (subsection III A), we consider the acoustic radiation of the pulsating sphere (subsection III B) and the calculation of the reflection/transmission undergone at an interface by a spherical wave (subsection III C).

II. THE ONE-DIMENSION CASE

As announced in the above introduction, we start the present study of the Lagrange picture with the simplest situation we may have to face: the one-dimension problem. Let us therefore consider a fluid occupying *at rest* a cylindrical volume with axis $\mathrm{O}x_0$ and section S (figure 2a), at equilibrium pressure P_0 and mass density ρ_0. Both ends, labeled $x_0 = 0$ and $x_0 = L$, are made of pistons that are supposed to be fixed. As displayed in figure 2, the slice of fluid comprised between the faces labeled x_0 and $x_0 + \mathrm{d}x_0$ has mass $\rho_0 S \mathrm{d}x_0$. At time t, its current thickness is (see figure 2b)

$$\big(x_0 + \mathrm{d}x_0 + u(x_0 + \mathrm{d}x_0, t)\big) - \big(x_0 + u(x_0, t)\big) = \left(1 + \frac{\partial u}{\partial x_0}\right)\mathrm{d}x_0, \tag{5a}$$

so that its current mass density is simply

$$\rho(x_0, t) = \frac{\rho_0}{1 + \dfrac{\partial u}{\partial x_0}}. \tag{5b}$$

Besides, within the framework of the Lagrange picture, the pressure forces undergone by this slice of fluid are respectively $SP_0(x_0, t)$ (left end) and $-\,SP(x_0 + \mathrm{d}x_0, t)$ (right end). Consequently, applying Newton's Second Law to the

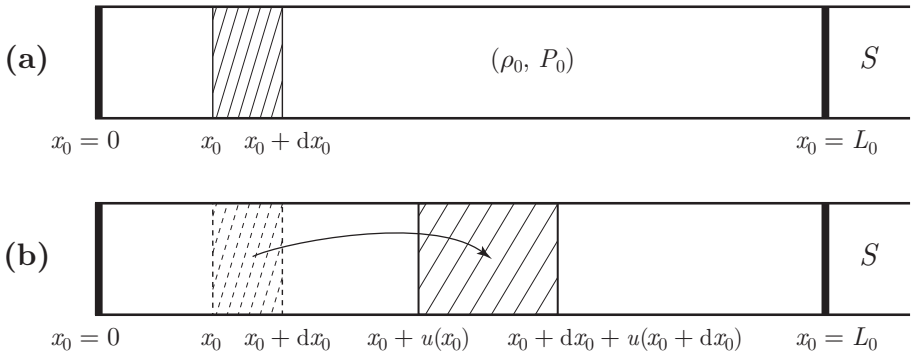

FIG. 2: (a). The fluid at rest, with equilibrium mass density ρ_0 and pressure P_0. (b). The fluid at time t. Both ends, labeled $x_0 = 0$ and $x_0 = L$, are made of fixed pistons.

latter slice, we obtain

$$\rho_0 \frac{\partial^{\mathcal{L}2} u}{\partial t^2} = -\frac{\partial P}{\partial x_0}, \tag{6}$$

where superscript $\mathcal{L}$ in the left-hand side recalls that the time-(second) derivative is understood at constant x_0 (even if the current position at time t of the face labeled "x_0" is quite away from the point with abscissa x_0 of the reference frame). The above equation (6) deserves at least a twofold comment: (*i*) it is *exact* (we made no approximation); (*ii*) it is *linear* in displacement u (or in velocity $v = \frac{\partial^{\mathcal{L}} u}{\partial t}$). Establishing equation (6) is half of the job. If we want now to get a propagation equation, we have to connect the pressure $P(x_0, t)$ with the expansion factor $\frac{\partial u}{\partial x_0}$ (or equivalently the mass density ρ). This is a thermodynamic issue. Throughout the present article, we shall assume, for the sake of simplicity, that any transformation undergone by the fluid is *isentropic*. In the framework of the Lagrange picture, this means that the entropy of any fluid slice $[x_0, x_0 + \mathrm{d}x_0]$ is, at any time, equal to its equilibrium value, so that in the course of the motion, the pressure $P(x_0, t)$ can be expressed as a function of the sole mass density $\rho(x_0, t)$ (let us recall that, in the Lagrange picture, the slice $[x_0, x_0 + \mathrm{d}x_0]$ does constitute a *closed* thermodynamic system). It will appear in the following discussion that it is most convenient to expand the extrapressure $p(x_0, t) = P(x_0, t) - P_0$ in increasing powers of $\frac{\partial u}{\partial x_0}$:

$$p(x_0, t) = -\kappa_1 \left(\frac{\partial u}{\partial x_0}\right) + \frac{1}{2}\kappa_2 \left(\frac{\partial u}{\partial x_0}\right)^2 + \cdots, \tag{7}$$

where the bulk modulus $\kappa_1 > 0$ due to the Second law of thermodynamics. Combining the mechanical equation (6) (in which the superscript $\mathcal{L}$ for "Lagrange" is henceforth omitted) with the above thermodynamic relation (7), we get the sound propagation equation

$$\rho_0 \frac{\partial^2 u}{\partial t^2} = \kappa_1 \frac{\partial^2 u}{\partial x_0^2} \left(1 - \frac{\kappa_2}{\kappa_1} \frac{\partial u}{\partial x_0} + \cdots\right). \tag{8}$$

The above equation is nonlinear in displacement u, its nonlinearity originating exclusively in the nonzero κ_2, κ_3, *etc.* coefficients in the thermodynamic expansion (7).

A. The linear approximation

We shall henceforth deliberately linearize the above equation (7), *i.e.* we assume that $\kappa_2 = \kappa_3 = \cdots = 0$. The propagation equation (8) becomes also linear, and reads

$$\frac{1}{c^2} \frac{\partial^2 u}{\partial t^2} = \frac{\partial^2 u}{\partial x_0^2}, \tag{9a}$$

with

$$c = \sqrt{\frac{\kappa_1}{\rho_0}}. \tag{9b}$$

Let us look for the acoustic eigenmodes, *i.e.* the monochromatic solutions of (9a). They necessarily read, owing to the boundary conditions we have choosen and $\Re$ denoting the real part,

$$u_n(x_0,t) = \Re\big\{A_n \sin(k_n x_0)\, \mathrm{e}^{-\mathrm{i}\omega_n t}\big\}, \tag{10a}$$

with

$$\omega_n = ck_n, \qquad k_n = \frac{n\pi}{L_0} \quad (n = 1, 2, \cdots), \tag{10b}$$

and A_n a (complex) amplitude. Note that, as far as the linearization of the *thermodynamic* relation (7) (*i.e.* $\kappa_2 = \kappa_3 = \cdots = 0$) is relevant, the above solution is *exact*, in contrast to the solution generally proposed in the framework of the Euler picture, which requires *in addition* the linearization of the Euler equation, *i.e.* neglecting the $(\vec{v}\cdot\overrightarrow{\mathrm{grad}})\,\vec{v}$ term in (2), namely (as recalled in the introduction) that the fluid particle velocities should be small compared to the wave phase velocity.

Let us now determine the overall acoutic energy associated with the wave, *i.e.* the variation (with respect to the rest state) of the sum of all the $[x_0, x_0+\mathrm{d}x_0]$ slices total energy. Since there is neither heat exchange between neighbouring slices nor external force, we just have to determine the (mechanical) work done by the pressure forces to drive each fluid slice from its equilibrium state to its current state at time t. For the $[x_0, x_0+\mathrm{d}x_0]$ slice, the energy variation is exactly

$$\begin{aligned}\mathrm{d}E &= \int_0^t \mathrm{d}t'\bigg[-SP(x_0+\mathrm{d}x_0,t')\frac{\partial u(x_0+\mathrm{d}x_0,t')}{\partial t'} + SP(x_0,t')\frac{\partial u(x_0,t')}{\partial t'}\bigg]\\ &= S\mathrm{d}x_0\int_0^t \mathrm{d}t'\bigg[-\frac{\partial P}{\partial x_0}\frac{\partial u}{\partial t'} - P\frac{\partial^2 u}{\partial x_0 \partial t'}\bigg].\end{aligned} \tag{11a}$$

Owing to (6) and to the linarized version of (7), the above equation becomes

$$\mathrm{d}E = S\mathrm{d}x_0\bigg[\frac{1}{2}\rho_0\bigg(\frac{\partial u(x_0,t)}{\partial t}\bigg)^2 - P_0\frac{\partial u(x_0,t)}{\partial x_0} + \frac{1}{2}\kappa_1\bigg(\frac{\partial u(x_0,t)}{\partial x_0}\bigg)^2\bigg]. \tag{11b}$$

Integrating over the whole fluid, and accounting for (9b) and our boundary conditions, we finally get the overall acoustic energy E, which is a constant of the movement:

$$E = \frac{1}{2}\rho_0 S\int_0^{L_0}\mathrm{d}x_0\bigg[\bigg(\frac{\partial u}{\partial t}\bigg)^2 + c^2\bigg(\frac{\partial u}{\partial x_0}\bigg)^2\bigg]. \tag{11c}$$

Now, since any solution $u(x_0,t)$ of the wave equation (9a) is but a linear combination of eigenmodes of the type (10a), the above energy (11c) may also be written, all calculations carried out,

$$E = \frac{1}{4}\rho_0 S L_0\sum_{n=1}^{\infty}|A_n|^2\omega_n^2. \tag{11d}$$

The above results deserve the following remark. Introducing the acoustic energy density

$$\mathcal{E} = \frac{\mathrm{d}E}{S\,\mathrm{d}x_0}, \tag{12a}$$

the time-derivative of (11a) reads

$$\frac{\partial\mathcal{E}}{\partial t} + \frac{\partial}{\partial x_0}\bigg(P\frac{\partial u}{\partial t}\bigg) = 0, \tag{12b}$$

and should be regarded as the Lagrange expression of the local acoustic energy conservation, $\mathcal{G} = P\frac{\partial u}{\partial t}$ standing for the (1D) acoustic Poynting vector. Observe that the energy density $\mathcal{E}$ is defined with respect to the *rest* volume (denominator $S\,\mathrm{d}x_0$ in (12a)). Likewise, the (one-dimension) divergence ($\partial/\partial x_0$ in (12b)) is expressed using the *rest* coordinate: $\mathcal{G}$ is derived with respect to the *label* x_0, not to the current spatial position x.

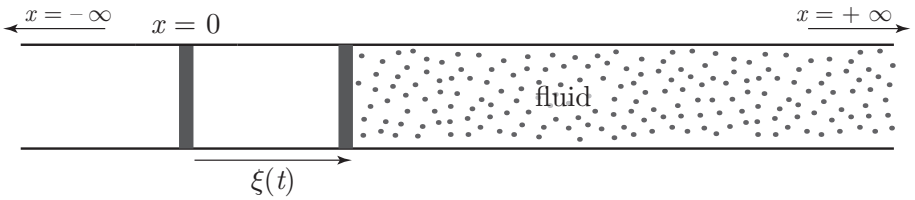

FIG. 3: A moving piston, with abscissa $\xi(t)$, generates an acoustic wave propagating towards $x = +\infty$.

B. The pulsating piston

Consider the situation illustrated in figure 3. A (1D) fluid occupies at rest and at the equilibrium pressure P_0 the $x > 0$ domain. A piston is placed at $x = 0$. Now, let the piston move (for instance pulsate around its rest position) and let $\xi(t)$ be its abscissa at time t.

How can we account for the motion of the fluid? The answer is most simple in the framework of the Lagrange picture. Since no wave is coming from $x = +\infty$, the relevant solution of equation (9a) reads

$$u(x_0, t) = f\Big(t - \frac{x_0}{c}\Big), \tag{13a}$$

where f is a regular function determined by imposing

$$u(x_0 = 0, t) = \xi(t) \ \ \forall t \quad \rightsquigarrow \quad f = \xi. \tag{13b}$$

Besides, using (7) in its linear form, we get

$$p(x_0, t) = \frac{\kappa_1}{c} f'\Big(t - \frac{x_0}{c}\Big) = Z v(x_0, t), \tag{14}$$

where $v(x_0, t) = \frac{\partial u(x_0,t)}{\partial t}$ is the velocity field of the fluid and

$$Z = \rho_0 c = \frac{\kappa_1}{c} = \sqrt{\kappa_1 \rho_0} \tag{15}$$

is its acoustic impedance. Observe by the way that the extrapressure exerted by the piston to move the fluid is $Z\dot{\xi}$, hence $\mathcal{G} = P_0\dot{\xi} + Z\dot{\xi}^2$: (in 1D geometry) the time average ($\langle\,\rangle$) acoustic power radiated by an oscillating ($\langle\dot{\xi}\rangle = 0$) piston is $Z\langle\dot{\xi}^2\rangle$ per unit (transverse) surface.

We leave it to the reader as a challenge to propose a simpler solution in the framework of the Euler picture.

C. Reflection/transmission at an interface

Let us now go back to the question raised in the introduction and show that the Lagrange picture provides an exact calculation of the reflection/transmission coefficients. Let us consider fig. 1 again. At rest, medium 1 and medium 2 are separated by the plane $x = 0$. Choosing the rest state of the system to implement the Lagrange labeling of the fluid elements, $x_0 = 0$ labels both the right-hand face of the last slice of medium 1, and the left-hand face of the first slice of medium 2. This labeling will "follow" the motion of the system and (provided of course that no mixing occurs between the two fluids) the Lagrange labeling of the interface will remain $x_0 = 0$ throughout the propagation of the acoustic wave, whatever the amplitude of the latter and without any approximation. Let ρ_{0j}, resp. κ_j, $(j = 1, 2)$ denote the rest mass density, resp. the bulk modulus, of medium j. According to (9b), $c_j = \sqrt{\kappa_j/\rho_{0j}}$ is the speed of sound in medium j. Let us consider an acoustic wave coming from $x = -\infty$. This incident wave is described by the displacement field $u_{\rm i}(x_0, t) = f\big(t - \frac{x_0}{c_1}\big)$, where f is any (regular) function. When the wave reaches the interface (labeled $x_0 = 0$, whatever its motion), it splits into a reflected wave $u_{\rm r}(x_0, t) = g\big(t + \frac{x_0}{c_1}\big)$ and a transmitted wave $u_{\rm t}(x_0, t) = h\big(t - \frac{x_0}{c_2}\big)$. In summary, the total displacement field u reads

$$\begin{aligned} &\text{for } x_0 < 0: \ u(x_0, t) = f\Big(t - \frac{x_0}{c_1}\Big) + g\Big(t + \frac{x_0}{c_1}\Big), \\ &\text{for } x_0 > 0: \ u(x_0, t) = h\Big(t - \frac{x_0}{c_2}\Big), \end{aligned} \tag{16a}$$

whereas the extrapressure field p reads, owing to the linearized version of (7):

$$\text{for } x_0 < 0 : \; p(x_0,t) = Z_1\left(f'\left(t-\frac{x_0}{c_1}\right) - g'\left(t+\frac{x_0}{c_1}\right)\right),$$
$$\text{for } x_0 > 0 : \; p(x_0,t) = Z_2 h'\left(t-\frac{x_0}{c_2}\right), \tag{16b}$$

where $Z_1 = \rho_{01}c_1 = \kappa_{11}/c_1 = \sqrt{\kappa_{11}\rho_{01}}$ and $Z_2 = \rho_{02}c_2 = \kappa_{12}/c_2 = \sqrt{\kappa_{12}\rho_{02}}$ stand for the acoustic impedances of media 1 and 2. Writing the continuities of v and p at the interface $x_0 = 0$ at any time t, we obtain the well-known reflection/transmission coefficient in *velocity*

$$r_v = \frac{g'}{f'} = \frac{Z_1 - Z_2}{Z_1 + Z_2}, \qquad t_v = \frac{h'}{f'} = \frac{2Z_1}{Z_1+Z_2} = 1 + r_v \tag{16c}$$

and in *extrapressure*

$$r_p = -\frac{g'}{f'} = -\,r_v, \qquad t_p = \frac{Z_2 h'}{Z_1 f'} = \frac{Z_2}{Z_1} t_v. \tag{16d}$$

In the framework of the linear thermodynamic response, the Lagrange picture thus provides the simplest quantitative description of the reflection/transmission phenomenon of an acoustic wave at an interface. Observe too that equalling the acoustic Poynting vectors on either side of the interface $x_0 = 0$, we recover the well known relation $R + T = 1$, where

$$R = -\,r_v r_p = \left(\frac{Z_1 - Z_2}{Z_1 + Z_2}\right)^2 \quad \text{and} \quad T = t_v t_p = \frac{4Z_1 Z_2}{(Z_1+Z_2)^2} \tag{17}$$

are the *power* reflection and transmission coefficients. It is noteworthy that, in 1D geometry, reflection and dispersion are nondispersive.

III. THE THREE-DIMENSION CASE

A. A quick overflight of the motion equations

Let us now come back to equation (6) and see how it can be generalized in the three-dimension case. Considering a fluid amount with (rest) volume $V_0 = \int \mathrm{d}\tau_0$ and (rest) mass density ρ_0, Newton's Second Law reads

$$\int \mathrm{d}\tau_0 \, \rho_0 \frac{\partial^2 \vec{u}}{\partial t^2} = \iint_{\Sigma(t)} -\,P \, \mathrm{d}\vec{s}, \tag{18a}$$

where $\Sigma(t)$ is the external surface of the fluid amount at time t (see figure 4), and P the actual pressure exerted onto this fluid amount by its surroundings. Using Ostrogradsky's theorem, the surface integral in the right-hand side of the above equation is changed in a volume integral

$$\iint_{\Sigma(t)} -\,P \, \mathrm{d}\vec{s} = \int \mathrm{d}\tau \, (-\overrightarrow{\mathrm{grad}}\, P) \tag{18b}$$

where $\mathrm{d}\tau$ is the volume at time t of the deformed fluid element whose volume was $\mathrm{d}\tau_0$ at rest. Introducing the dilatation factor

$$J = \frac{\mathrm{d}\tau}{\mathrm{d}\tau_0} \tag{19a}$$

(J is the jacobian of the variable change $\vec{r}_0 \rightsquigarrow \vec{r}$ displayed in (3)), it can be shown and we leave it to the reader to check that

$$\frac{\partial J}{\partial t} = J \, \mathrm{div}\, \vec{v}. \tag{19b}$$

Therefore, an incompressible flow corresponds to $\mathrm{div}\, \vec{v} = 0$, exactly like in the framework of the Euler picture.

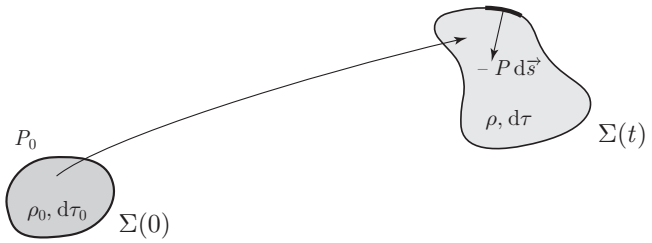

FIG. 4: An amount of fluid with rest mass density ρ_0 and wrapped in its (external) surface $\Sigma(0)$ under the (rest) pressure P_0 is displaced and deformed in the course of the motion. At time t, it undergoes the outside pressure P exerted onto its (external) surface $\Sigma(t)$.

Since the above equations (18a) and (18b) hold whatever the integration volume, we are left with the local motion equation

$$\rho_0 \frac{\partial^2 \vec{u}}{\partial t^2} = -\,J \overrightarrow{\mathrm{grad}}\, P, \tag{20}$$

where superscript "$\mathcal{L}$" (for "Lagrange") is understood in the left-hand side time-derivative.

The above motion equation obtained in the Lagrange picture is nonlinear (due to J in the right-hand side). It is interestingly compared to the Euler equation recalled in (2). To begin with, let us observe that the fluid velocity $\vec{v}$ is nothing else than the (Lagrange) time-derivative of the displacement $\vec{u}$. Restoring provisionally superscripts "$\mathcal{L}$" and "$\mathcal{E}$", we have indeed

$$\frac{\partial^{\mathcal{L}} \vec{u}}{\partial t} = \vec{v} \tag{21a}$$

and

$$\frac{\partial^{\mathcal{L}2} \vec{u}}{\partial t^2} = \frac{\partial^{\mathcal{L}} \vec{v}}{\partial t} = \frac{\partial^{\mathcal{E}} \vec{v}}{\partial t} + \big(\vec{v} \cdot \overrightarrow{\mathrm{grad}}\big)\vec{v}. \tag{21b}$$

Moreover, observing that the fluid mass density ρ is (as a consequence of (19a) for instance) equal to ρ_0/J, we conclude that equations (2) and (20) are perfectly equivalent.

Interesting too is the comparison between the three-dimension motion equation (20) and its one-dimension reduced expression (6). A (too) quick glance may instil the uncomfortable – and misleading – feeling that the J factor has disappeared from the right-hand side of (6). In fact, in the one-dimension problem considered in section II, if x_0 and x respectively denote the abscissa at rest and at time t of the same fluid element (therefore labeled x_0), we have, owing for (19a),

$$\mathrm{grad} = \frac{\partial}{\partial x} = \frac{1}{J}\frac{\partial}{\partial x_0}, \tag{22a}$$

hence (20) becomes, in the one-dimension case,

$$\rho_0 \frac{\partial^2 \vec{u}}{\partial t^2} = -\,J \overrightarrow{\mathrm{grad}}\, P = -\,J\,\frac{\partial P}{\partial x} = -\,\frac{\partial P}{\partial x_0}, \tag{22b}$$

so that (6) is recovered. In the same connection, it is not difficult to extend the results of equations (11a-d) to the three-dimension case and set out the energy balance in the Lagrange picture, as explained below.

Let us consider the fluid amount displayed in figure 4, and let E be its total energy. For the sake of simplicity, we assume here again that there is no external force (gravity or other) acting on the fluid. Since the transformations of the latter fluid are supposed to be isentropic, the time variations of E are (exactly as in the 1D case) only due to the work of the outer pressure forces exerted upon surface $\Sigma(t)$:

$$\frac{\mathrm{d}E}{\mathrm{d}t} = \iint_{\Sigma(t)} -\,P\,\mathrm{d}\vec{s} \cdot \frac{\partial \vec{u}}{\partial t}, \tag{23a}$$

entailing (through Ostrogradsky's theorem)

$$\frac{\mathrm{d}E}{\mathrm{d}t} + \int \mathrm{d}\tau \,\mathrm{div}\,\vec{\mathcal{G}} = 0, \tag{23b}$$

where $\vec{\mathcal{G}} = P\dfrac{\partial \vec{u}}{\partial t}$ is the so-called acoustic Poynting vector. Detailing the above energy conservation equation, we get, owing to (19a), (19b) and (20),

$$\begin{aligned} \frac{\mathrm{d}E}{\mathrm{d}t} &= -\int \mathrm{d}\tau \left[\overrightarrow{\mathrm{grad}}\, P \cdot \frac{\partial \vec{u}}{\partial t} + P\,\mathrm{div}\,\frac{\partial \vec{u}}{\partial t}\right] = -\int \mathrm{d}\tau_0 \left[J\overrightarrow{\mathrm{grad}}\, P \cdot \frac{\partial \vec{u}}{\partial t} + PJ\,\mathrm{div}\,\frac{\partial \vec{u}}{\partial t}\right] \\ &= \int \mathrm{d}\tau_0 \left[\rho_0 \frac{\partial^2 \vec{u}}{\partial t^2} \cdot \frac{\partial \vec{u}}{\partial t} - P\frac{\partial J}{\partial t}\right], \end{aligned} \tag{24a}$$

where $\int \mathrm{d}\tau$, resp. $\int \mathrm{d}\tau_0$, denote integrals over the volumes occupied at current time t, resp. at rest, by the amount of fluid shown in figure 4. Equation (24a) consequently reads

$$\frac{\mathrm{d}E}{\mathrm{d}t} = \frac{\mathrm{d}E_\mathrm{k}}{\mathrm{d}t} + \mathcal{P}_\mathrm{c}, \tag{24b}$$

where $E_\mathrm{k} = \displaystyle\int \mathrm{d}\tau_0 \,\frac{1}{2}\rho_0 \left(\frac{\partial \vec{u}}{\partial t}\right)^2$ is the overall kinetic energy and $\mathcal{P}_\mathrm{c} = \displaystyle\int \mathrm{d}\tau_0 \left(-P\frac{\partial J}{\partial t}\right)$ is the overall compression power of the pressure forces undergone by the fluid. As a matter of fact, due to the absence of any thermal exchange, equation (24b) is but the expression of the First Principle of Thermodynamics. As was already the case in 1D geometry, calculating the latter compression power is a thermodynamic issue which requires the P-versus-J relation. We have indeed $P\frac{\partial J}{\partial t} = \frac{\mathrm{d}}{\mathrm{d}t}\int_1^J P(J')\,\mathrm{d}J'$, hence, since the integral $\int \mathrm{d}\tau_0$ concerns a time-independent integration volume,

$$\mathcal{P}_\mathrm{c} = \frac{\mathrm{d}}{\mathrm{d}t}\int \mathrm{d}\tau_0 \int_1^J -P(J')\mathrm{d}J'. \tag{25}$$

In the particular case of a linear thermodynamic response of the type

$$p = P - P_0 = -\kappa_1 (J-1), \tag{26a}$$

setting $\kappa_1 = \rho_0 c^2$ like in (9b), we are left, all calculations carried out, with

$$E + P_0(V - V_0) = \frac{1}{2}\int \mathrm{d}\tau_0\, \rho_0 \left[\left(\frac{\partial \vec{u}}{\partial t}\right)^2 + c^2 (J-1)^2\right], \tag{26b}$$

where V and V_0 are the overall volume of the fluid, respectively at current time t and at rest. Observe that, in the framework of the *small* deformation approximation (26a), the expansion term $J-1$ should be substituted by $\mathrm{div}\,\vec{u}$. In the latter framework, the above result (26b) thus generalizes (11c). Observe too that, in the case where the fluid undergoes an outer pressure P_0, the quantity $E + P_0(V - V_0)$, and hence the enthalpy, is conserved in the course of time.

B. The pulsating sphere

The well known problem of the acoustic wave generated by a pulsating sphere will illustrate the convenience of the Lagrange picture. Let us consider an infinite homogeneous elastic fluid. A pulsating sphere, with center at the origin of a spherical coordinate system and with current radius $R(t) = R_0 + \xi(t)$, excitates spherical waves in the fluid (see figure 5a). For the sake of simplicity, let us restrict our study to the small deformation limit. Due to the spherical symmetry of the motion, all relevant quantities (pressure, temperature) are independent of angles θ and φ. The displacement field $\vec{u}$ reads

$$\vec{u}(\vec{r}, t) = u(r, t)\vec{e}_r, \tag{27a}$$

where $\vec{e}_r$ is the radial unitary vector of the spherical coordinate system. Thus, linearizing equation (20), we get the simple motion equation

$$\rho_0 \frac{\partial^2 u}{\partial t^2} = -\frac{\partial P}{\partial r} = -\frac{\partial p}{\partial r}. \tag{27b}$$

Assuming a linear *p-versus-*$(J-1)$ thermodynamic relation of the type (26a) and linearizing the expansion term $J-1$, we obtain the extrapressure

$$p = -\kappa_1 \mathrm{div}\,\vec{u} = -\frac{\kappa_1}{r^2}\frac{\partial(r^2 u)}{\partial r}. \tag{28a}$$

From the above expression, the d'Alembert wave equation

$$\left(\frac{1}{c^2}\frac{\partial^2}{\partial t^2} - \frac{\partial^2}{\partial r^2}\right)\big(rp(r,t)\big) = 0 \tag{28b}$$

is obtained. The mathematical treatment of this equation is well known from textbooks. Since there is no incoming spherical wave from infinity, its general relevant solution is

$$p(r,t) = \frac{1}{r}\varphi\left(t - \frac{r-R_0}{c}\right), \tag{29}$$

where φ is any (regular) function. Choosing the Lagrange picture reveals its convenience *in fine* when one has to determine function φ knowing the motion $\xi(t)$ of the pulsating sphere, as shown below. Using (29) to rewrite the right-hand side of (27b), we get

$$\rho_0\frac{\partial^2 u}{\partial t^2} = \frac{1}{r^2}\varphi\left(t - \frac{r-R_0}{c}\right) + \frac{1}{rc}\varphi'\left(t - \frac{r-R_0}{c}\right) = \frac{1}{r^2}\left(1 + \frac{r}{c}\frac{\mathrm{d}}{\mathrm{d}t}\right)\varphi\left(t - \frac{r-R_0}{c}\right). \tag{30a}$$

Simply equalizing $u(r=R_0,t)$ and $\xi(t)$ we obtain the differential equation

$$\rho_0\ddot{\xi} = \frac{1}{R_0^2}\left(1 + \frac{R_0}{c}\frac{\mathrm{d}}{\mathrm{d}t}\right)\varphi(t), \tag{30b}$$

the solution of which we symbolically denote

$$\varphi(t) = \rho_0 R_0^2\left(1 + \frac{R_0}{c}\frac{\mathrm{d}}{\mathrm{d}t}\right)^{(-1)}\ddot{\xi}(t). \tag{30c}$$

Allowing for (29) and (30c) we get the extrapressure $p(r,t)$. On the other hand, owing to (30c) again and after a (double) time-integration of (30a), we get the symbolic expression of the displacement

$$u(r,t) = \frac{R_0^2}{r^2}\left(1 + \frac{R_0}{c}\frac{\mathrm{d}}{\mathrm{d}t}\right)^{(-1)}\left(1 + \frac{r}{c}\frac{\mathrm{d}}{\mathrm{d}t}\right)\xi\left(t - \frac{r-R_0}{c}\right). \tag{31}$$

At this step, it is interesting to consider the following two limit-situations.

(*i*) $\frac{R_0}{c}|\dot{\xi}| \gg |\xi|$. In the case of a monochromatic pulsation of the sphere, the condition $\frac{R_0\omega}{c} \gg 1$ means that the wavelength of the generated acoustic wave is *small* compared to radius R_0. Neglecting unity with respect to $\frac{R_0}{c}\frac{\mathrm{d}}{\mathrm{d}t}$ in (30c), we simply get

$$\varphi \simeq \rho_0 c R_0 \dot{\xi}, \tag{32a}$$

and consequently

$$u(r,t) \simeq \frac{R_0}{r}\xi\left(t - \frac{r-R_0}{c}\right), \quad p(r,t) \simeq \frac{R_0}{r}\rho_0 c\dot{\xi}\left(t - \frac{r-R_0}{c}\right) = Zv(r,t), \tag{32b}$$

which (save for the $\frac{R_0}{r}$ prefactor characteristic of the 3D geometry) is exactly what was expected from the 1D analysis in subsection II B (see (13)-(15)). The total acoutic power radiated by the pulsating sphere is thus

$$\mathcal{P}(t) = 4\pi R_0^2\mathcal{G}(R_0,t) = 4\pi R_0^2 Z\dot{\xi}^2. \tag{32c}$$

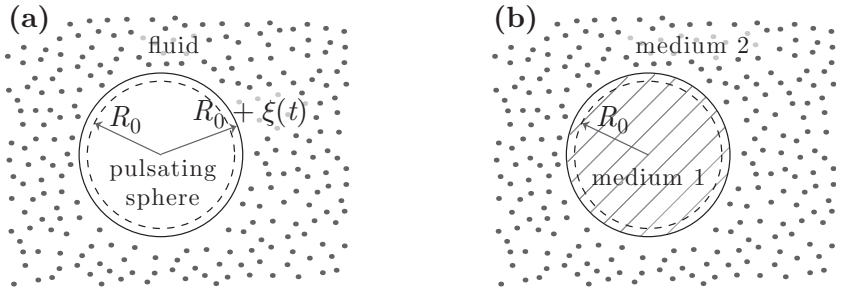

FIG. 5: (a). A pulsating sphere with current radius $R(t) = R_0 + \xi(t)$ generates an outgoing spherical wave in the outer fluid. (b). Medium 1 and medium 2 are separated at rest by a spherical interface with radius R_0 (dashed line) and center at the origin. An outgoing spherical pressure wave, generated in the $r < R_0$ area, is reflected/transmitted at the interface.

(*ii*) $\frac{R_0}{c}|\dot{\xi}| \ll |\xi|$. In the case of a monochromatic pulsation of the sphere, the condition $\frac{R_0\omega}{c} \ll 1$ means that the wavelength of the generated acoustic wave is *large* compared to radius R_0. Solution (30c) can then be expanded as a series of time-derivatives of $\ddot{\xi}$, yielding

$$\varphi \simeq \rho_0 R_0^2 \left(\ddot{\xi} - \frac{R_0}{c} \dddot{\xi} + \cdots \right), \tag{33a}$$

hence the extrapressure $p(r,t)$ (using (29)) and the displacement

$$u(r,t) = \left[\frac{R_0^2}{r^2}\xi + \frac{R_0^2}{r^2}\left(1 - \frac{R_0}{r}\right)\left(\dot{\xi} - \frac{R_0}{c}\ddot{\xi} + \cdots \right) \right] \left(t - \frac{r - R_0}{c} \right). \tag{33b}$$

Observe that, in the present limit-situation (*ii*), the extrapressure is dominated by $\ddot{\xi}$, instead of $\dot{\xi}$ in (*i*), and that the part of the displacement proportional to ξ decays like $1/r^2$, instead of $1/r$ in (*i*). The power $\mathcal{P}(t)$ furnished by the sphere to move the fluid reads, setting $M = 4\pi\rho_0 R_0^3$,

$$\mathcal{P}(t) = 4\pi R_0^2 \mathcal{G}(R_0, t) = M \left(\ddot{\xi} - \frac{R_0}{c} \dddot{\xi} \right) \dot{\xi}. \tag{34a}$$

It is noteworthy that the first term in the right-hand side of the above equation simply reads $\frac{\mathrm{d}}{\mathrm{d}t}\left(\frac{1}{2}M\dot{\xi}^2\right)$: the $\ddot{\xi}$ term in the extrapressure accounts for a renormalization of the mass of the pulsating sphere. The $\dddot{\xi}$ term accounts for an acoustic radiated power

$$\langle \mathcal{P} \rangle = -M \frac{R_0}{c} \langle \dddot{\xi}\, \dot{\xi} \rangle = 4\pi\rho_0 \frac{R_0^4}{c} \langle \ddot{\xi}^2 \rangle. \tag{34b}$$

Note too that the behavior of the pulsating sphere in the (*ii*) limit-situation is quite analogous to that of moving charges in electrodynamics, the $\dddot{\xi}$ term in equations (33a) and (34a-b) bearing the equivalent of the Abraham-Lorentz force.[6]

C. Reflection/transmission in a spherical geometry

The formalism used in the above subsection III B also offers the opportunity to determine the reflection and transmission coefficients of an acoustic wave at the interface between the two media (1 and 2) considered in subsection II C, but now in spherical geometry. Let us consider figure 5b. An outgoing spherical wave is supposed to propagate in medium 1. This wave reaches a spherical interface with *rest* radius R_0. It is then split in a reflected wave and a transmitted wave. Disregarding further possible reflection at the origin, the pressure field is described (in the linear approximation) by

$$r < R_0 : \; p(r,t) = \frac{1}{r}\left[\varphi\left(t - \frac{r - R_0}{c_1} \right) + \gamma\left(t + \frac{r - R_0}{c_1} \right) \right] \tag{35a}$$

$$r > R_0 : \; p(r,t) = \frac{1}{r}\eta\left(t - \frac{r - R_0}{c_2} \right). \tag{35b}$$

Equalizing the pressures at the interface (labeled $r = R_0$) we naturally get

$$\varphi(t) + \gamma(t) = \eta(t). \tag{36a}$$

Equalizing the accelerations of the fluid at this interface $r = R_0$, we also get (see (30a) for instance)

$$\frac{1}{\rho_{01}}\left[\frac{1}{R_0}\big(\varphi(t)+\gamma(t)\big) + \frac{1}{c_1}\big(\varphi'(t)-\gamma'(t)\big)\right] = \frac{1}{\rho_{02}}\left[\frac{1}{R_0}\eta(t) + \frac{1}{c_2}\eta'(t)\right]. \tag{36b}$$

Contrary to its 1D analogous discussed in subsection II C, the above system cannot be simply solved for $\gamma(t)$ and $\eta(t)$. This is due to the mixing, in equation (36b), of funtions φ, γ, η with their time-derivatives φ', γ', η', which accounts for dispersive reflection and transmission of the wave at the interface. Considering indeed a monochromatic solution of the above equations (36a-b) and setting $\varphi(t) = \Re[\tilde{\varphi}\,\mathrm{e}^{-\mathrm{i}\omega t}]$, $\gamma(t) = \Re[\tilde{\gamma}\,\mathrm{e}^{-\mathrm{i}\omega t}]$ and $\eta(t) = \Re[\tilde{\eta}\,\mathrm{e}^{-\mathrm{i}\omega t}]$, we are left with the relations

$$\tilde{\varphi} + \tilde{\gamma} = \tilde{\eta} \tag{37a}$$

$$\frac{\tilde{\varphi}}{z_1} - \frac{\tilde{\gamma}}{z_1^*} = \frac{\tilde{\eta}}{z_2}, \tag{37b}$$

where, setting $k_1 = \omega/c_1$ and $k_2 = \omega/c_2$,

$$\frac{1}{z_1} = \frac{1}{Z_1}\left(1 + \frac{\mathrm{i}}{k_1 R_0}\right), \quad \frac{1}{z_2} = \frac{1}{Z_2}\left(1 + \frac{\mathrm{i}}{k_2 R_0}\right) \tag{38}$$

stand for complex effective acoustic impedances at the interface $r = R_0$. Observe that for k_1R_0, $k_2R_0 \gg 1$ (*i.e.* interface radius large compared to the acoustic wavelengths) z_1 and z_2 are real, and coincide with the usual impedances Z_1 and Z_2 introduced in subsection II C. From the above system (37a-b) one can easily derive the reflection and transmission coefficients in *extrapressure*

$$r_p = \frac{\tilde{\gamma}}{\tilde{\varphi}} = \frac{\dfrac{1}{z_1} - \dfrac{1}{z_2}}{\dfrac{1}{z_1^*} + \dfrac{1}{z_2}}, \quad t_p = \frac{\tilde{\eta}}{\tilde{\varphi}} = 1 + r_p, \tag{39a}$$

in *velocity*

$$r_v = -\frac{z_1}{z_1^*} r_p, \quad t_v = 1 + r_v = \frac{z_1}{z_2} t_p, \tag{39b}$$

and in *power*

$$R = |r_p^2|, \quad T = \frac{Z_1}{Z_2}|t_p|^2, \tag{39c}$$

to be compared with the 1D results (16c-d) and (17).

Considering figure 5b again, we can also envisage the case where an incoming spherical wave propagates in medium 2 (from infinity). When it reaches the interface, it splits into a reflected wave (which goes back to infinity in medium 2) and a transmitted wave (which enters into medium 1). We leave it to the reader to check that the corresponding reflection and transmission coefficients can then be derived from expressions (39a-c) by simply permuting indices 1 and 2 and complex-conjugating the whole. In the latter case of the reflection of an incoming wave, it is interesting to consider the limit-situation $R_0 \to 0$. As shown by (38), both effective impedances z_1 and z_2 are then purely imaginary and tend towards zero. It is also noteworthy that *both* r_p and r_v tend towards -1 (as expected since t_p and t_v tend towards 0). This behavior is characteristic of the (3D) spherical geometry: in 1D, r_p and r_v are always opposite (see (16d)). A rather spectacular feature of the latter 3D geometry originates in the reflection dispersivity, as illustrated below. Let us consider an air bubble, with (rest) radius R_0, immersed in water. As far as spherical pressure waves are concerned, this system can be regarded as an acoustic cavity of Pérot-Fabry type, the sound bouncing between $r = 0$ (reflection coefficient = –1) and $r = R_0$ (reflection coefficient = $r_p(R_0)$). The amplitude of the wave inside the air cavity (medium 1) is then proportional to the infinite series

$$1 - r_p(R_0)\,\mathrm{e}^{2\mathrm{i}k_1R_0} + r_p^2(R_0)\,\mathrm{e}^{4\mathrm{i}k_1R_0} + \cdots = \frac{1}{1 + r_p(R_0)\,\mathrm{e}^{2\mathrm{i}k_1R_0}} = \frac{1}{D}. \tag{40}$$

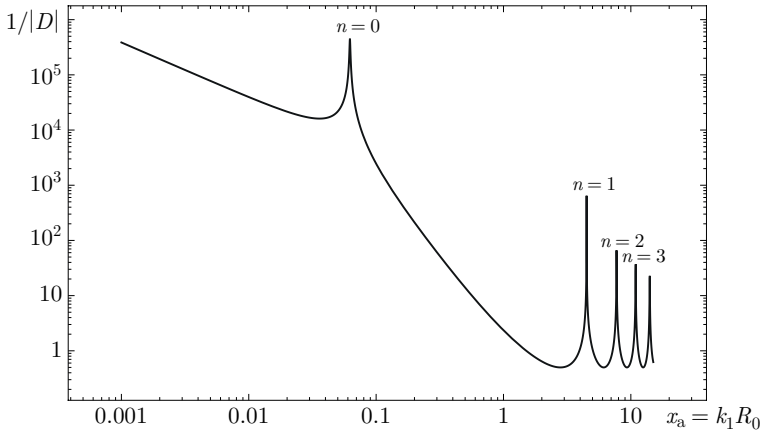

FIG. 6: The inverse absolute value of denominator D introduced in the text (see (40)) as a function of $x_\mathrm{a} = k_1 R_0$. The peaks of $|D^{-1}|$ correspond to the radial Pérot-Fabry acoustic resonances of the air bubble. Note that a log-log scale is necessary to display both the fundamental frequency peak and the others: for an air bubble at standard pressure and temperature, the fundamental resonance is obtained for $x_\mathrm{a} \simeq 6.2 \times 10^{-2} \ll \frac{\pi}{2}$ and its height is several orders of magnitude larger than that of the other peaks.

The resonances of the cavity naturally correspond to the minima of $|D|$. If the formulas (16c-d) of the 1D geometry were available in the present case, the reflection coefficient $r_p(R_0)$ would not depend of frequency. Moreover, with air as medium 1 and water as medium 2, the latter coefficient would be real and positive ($\simeq 1$ under the circumstances, since $Z_2 \simeq 5000\, Z_1$). As a consequence, $|D|^{-1}$ would display a series of equidistant peaks corresponding to $k_1 R_0 = (n + \frac{1}{2})\pi$ ($n = 0, 1, 2, \dots$). This is indeed what is obtained for $n \gg 1$: for higher-order resonances, the acoustic wavelengths (in air and *a fortiori* in water) are small compared to R_0 and the 1D results are available. But for low-order resonances ($n = 0$ or 1), the frequency-dependence of $r_p(R_0)$ entails both a "red shift" and an enhancement of the peaks, so much so that a log-log scale is necessary to display the lowest five resonances in figure 6. The shift of the fundamental resonance is tremendous. To derive it analytically, let us assume $k_1 R_0$, $k_2 R_0 \ll 1$ and expand denominator D in increasing powers of $x_\mathrm{a} = k_1 R_0$. Allowing for (38) and (39-a) we get, owing to $\rho_{01} \ll \rho_{02}$, $Z_1 \ll Z_2$,

$$D \simeq 2\mathrm{i} x_\mathrm{a} \left(\frac{\rho_{01}}{\rho_{02}} - \frac{x_\mathrm{a}^2}{3} \right) + o(x_\mathrm{a}^5). \tag{41}$$

As a consequence, the absolute value of denominator D has its lowest frequency minimum for

$$x_\mathrm{a}^2 \simeq \frac{3\rho_{01}}{\rho_{02}} \quad \rightsquigarrow \quad \omega = \omega_\mathrm{M} = \frac{c_1}{R_0} \sqrt{\frac{3\rho_{01}}{\rho_{02}}} = \sqrt{\frac{3\gamma P_0}{\rho_{02} R_0^2}}, \tag{42}$$

where P_0 is the pressure of the air inside the bubble and $\gamma = C_P/C_V$ the air heat capacities ratio. The story of the above formula (42) is worth relating. At the begining of the last century, to interpret the sound of the running water, R. Paget suggested that the fall of simple drops could generate air cavities oscillating much like resonators.[7] M. Minnaert objected that, for air bubbles with radii in the millimetric range, rigid-wall Pérot-Fabry resonances would correspond to frequencies overshooting the human ear sensitivity cutoff. Indeed, as mentioned above, the lowest fundamental resonance would be found, if the 1D results were available, for $x_\mathrm{a} \simeq \frac{\pi}{2}$, namely $f \simeq c_1/4R_0 \simeq 85$ kHz for $R_0 = 1$ mm. He then proposed an utterly different approach in a pioneering work,[8] and derived formula (42), ω_M being since known as the Minnaert angular frequency. At atmopheric pressure, for $R_0 = 1$ mm and $\gamma = 1.4$, the Minnaert frequency is $\omega_\mathrm{M}/2\pi \simeq 3.3$ kHz. Surprising though it may be, the Paget and the Minnaert interpretations are both correct, the controversy between them simply originates in their disregarding the peculiar behavior of the acoustic reflection/transmission at a spherical interface.

IV. CONCLUSION

In the present paper, we have argued that as far as acoustic propagation in fluids is considered, the Lagrange picture provides a very intuitive framework to carry out the calculations. This is particularly true in 1D geometry: provided

that the thermodynamic extrapressure-to-dilatation relation is linear, the motion equation itself is linear and can be solved without any approximation. Moreover, when the fluid is assigned a moving boundary condition (for instance when it is moved, like in subsection II B, by a pulsating piston), the Lagrange picture provides the most natural framework to account for this boundary condition. In 3D geometry, the motion equation of the fluid is no longer linear, unless the small movements approximation is made. Nevertheless the Lagrange picture remains convenient as concerns moving boundary conditions, as illustrated by the example of the pulsating sphere and related topics.

We thank Professor Jean-Claude Bacri for drawing our attention onto the air bubble problem.

---

* Electronic address: martin.devaud@univ-paris-diderot.fr

[1] L. D. Landau and E. M. Lifshitz, *Fluid Mechanics* (Pergamon Press, 1959).
[2] G. K. Batchelor, *An Introduction to Fluid Dynamics* (Cambridge University Press, 1970).
[3] P. M. Morse and K. U. Ingard, *Theoretical Acoustics* (Princeton University Press, 1986).
[4] É. Guyon, J.-P. Hulin, and L. Petit, *Hydrodynamique Physique* (EDP Sciences, CNRS Éditions, 2001).
[5] A. Bennett, *Lagrangian Fluid Dynamics* (Cambridge University Press, 2006).
[6] J. D. Jackson, *Classical Electrodynamics* (John Wiley and Sons, 1999).
[7] S. R. Paget (1921), cited by Sir W. Bragg in The world of sound, London.
[8] M. Minnaert, Phil. Mag. **6**, 235 (1933).